Femtochemistry

International Edition: DOI: 10.1002/anie.201507524
German Edition: DOI: 10.1002/ange.201507524

Microhydration Effects on the Ultrafast Photodynamics of Cytosine: Evidences for a Possible Hydration-Site Dependence

*Jr-Wei Ho, Hung-Chien Yen, Hui-Qi Shi, Li-Hao Cheng, Chih-Nan Weng, Wei-Kuang Chou, Chih-Chung Chiu, and Po-Yuan Cheng**

Abstract: *Ultrafast excited-state deactivation dynamics of small cytosine (Cy) and 1-methylcytosine (1mCy) microhydrates, $Cy\cdot(H_2O)_{1\text{-}3}$ and $1mCy\cdot(H_2O)_{1,2}$, produced in a supersonic expansion have been studied by mass-selected femtosecond pump–probe photoionization spectroscopy at about 267 nm excitation. The seeded supersonic expansion of Ar/H_2O gas mixtures allowed an extensive structural relaxation of Cy and 1mCy microhydrates to low-energy isomers. With the aid of electronic structure calculations, we assigned the observed ultrafast dynamics to the dominant microhydrate isomers of the amino-keto tautomer of Cy and 1mCy. Excited-state lifetimes of $Cy\cdot(H_2O)_{1\text{-}3}$ measured here are 0.2–0.5 ps. Comparisons of the $Cy\cdot H_2O$ and $1mCy\cdot H_2O$ transients suggest that monohydration at the amino Watson–Crick site induces a substantially stronger effect than at the sugar-edge site in accelerating excited-state deactivation of Cy.*

Hydrogen (H) bonds hold complementary nucleobases together in DNA to form the double helical structure. How the H-bonding interaction influences the intrinsic properties of nucleobases, for example the photostability arising from the short-lived nature of their excited-states,[1–3] remains an interesting and challenging question. Each nucleobase possesses multiple H-bonding sites, and therefore, it is intuitive to ponder if those involved in the Watson–Crick base pairing exhibit distinctive effects than the others.[4,5] Because water is an integral part of DNA biological structure and function,[6,7] it is also essential to understand how hydration affects the photostability of nucleobases at the molecular level. This work addresses these issues by studying the effect of H-bonding between water and an isolated nucleobase, cytosine (Cy), on its excited-state dynamics in stepwise microhydration.

In the gas phase, Cy exists in three major tautomeric forms, the amino-keto, amino-enol and imino-keto, hereafter referred to as the keto, enol, and imino forms (see Figure 1), respectively.[8–12] We have previously used femtosecond pump–probe photoionization spectroscopy to identify intrinsic excited-state dynamics of these Cy tautomers.[12] Our results indicated that, upon photoexcitation into their first $^1\pi\pi^*$ excited states, imino- and keto-Cy decay with sub-picosecond dynamics for $\lambda_{ex} < 300$ nm, whereas enol-Cy decays in 3 to 45 ps for excitations between 260 and 285 nm. These results are consistent with more recent experimental and theoretical works.[13–16] For example, it has been shown that the S_1-state lifetimes of keto-Cy are a few tens of picoseconds near the origin (ca. 314 nm) but drop sharply to 1–2 ps at 530 cm^{-1} above the S_1 zero point,[16] consistent with the sub-picosecond lifetimes measured at higher excitation energies.[12,17] In contrast, in aqueous solutions Cy exists exclusively in the keto form, and the first $^1\pi\pi^*$ excited state exhibits dynamics ranging from sub-picosecond to a few picoseconds.[1,2,18,19]

Here, we extend our study to examine small Cy water clusters, $Cy\cdot(H_2O)_{1\text{-}3}$. The experimental setup is similar to that employed previously,[12] and the details are given in the Supporting Information. Briefly, we excited Cy and its water clusters with femtosecond laser pulses at 267 nm, and the excited-state dynamics was monitored by measuring the multiphoton ionization yield at the mass channel of interest with delayed probe pulses at 800 nm. The experiments were carried out in a molecular beam apparatus equipped with a time-of-flight mass spectrometer. To produce $Cy\cdot(H_2O)_n$, a gas mixture of Ar containing 12 % of water vapor was allowed to flow through an oven containing Cy crystal at 490 K and then expanded through a 100 μm diameter pinhole to produce a continuous supersonic jet. The total stagnation pressure was about 400 torr, and the nozzle was kept at a slightly higher temperature (ca. 500 K) to avoid clogging.

Figure 1 A shows the pump–probe photoionization transients of Cy and $Cy\cdot(H_2O)_{1\text{-}3}$. Only small $Cy\cdot(H_2O)_n$ cluster ions ($n \leq 4$) were observed in the mass spectra when these transients were recorded (see the Supporting Information). Further reductions in water concentration as well as laser pulse energies did not change the decay profiles, suggesting that ionic fragmentation of larger clusters is not important. This is also supported by the fact that single-photon ionization of $Cy\cdot(H_2O)_{1\text{-}3}$ up to 10.5 eV did not show clear evidences for fragmentation.[20,21] The Cy monomer transient (trace a) is similar to that reported previously.[12] It contains an initial spike and other decay components that can be attributed to Cy major tautomers. The initial spike is mainly due to nonresonant pump–probe multiphoton ionization occurring only at time zero, and therefore, is irrelevant to the excited-state dynamics (see the Supporting Information).[12] For Cy monomer, theories and experiments have shown that the enol form is more stable than the keto by 3 kJ mol^{-1}.[8–12] However, structural relaxation during expansion is hindered by high barriers of 150–175 kJ mol^{-1} that separates Cy tautomers,[22–25] making their populations frozen at the temperature prior to

[*] Dr. J. W. Ho, H. C. Yen, H. Q. Shi, L. H. Cheng, C. N. Weng, W. K. Chou, Dr. C. C. Chiu, Prof. P. Y. Cheng
Department of Chemistry, National Tsing Hua University
Hsinchu, Taiwan 30043 (R.O.C.)
E-mail: pycheng@mx.nthu.edu.tw

Supporting information for this article is available on the WWW under http://dx.doi.org/10.1002/anie.201507524.

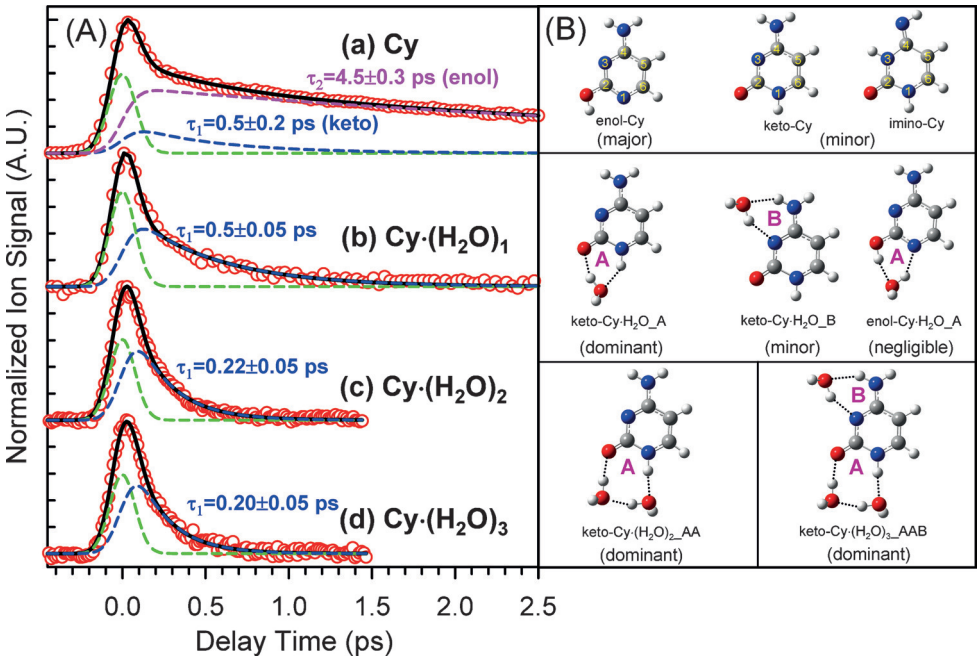

Figure 1. A) Mass-selected pump–probe photoionization transients (λ_{pump} = 267 nm; λ_{probe} = 800 nm) of Cy and Cy microhydrates: a) Cy monomer, b) Cy·H_2O, c) Cy·$(H_2O)_2$, and d) Cy·$(H_2O)_3$. The black solid lines are the best fits with a single-exponential (multi-exponential for the monomer) decay and an initial spike convoluted with the IRF (0.2 ps FWHM Gaussian). The dashed lines are the individual components obtained from the fits. B) Top panel: Chemical structures of the three major tautomers of Cy. Middle panel: ωB97XD-optimized structures of the three lowest-energy isomers of Cy·H_2O. Bottom panel: ωB97XD-optimized structures of the lowest-energy isomers of Cy·$(H_2O)_2$ and Cy·$(H_2O)_3$.

expansion (ca. 500 K). As concluded previously,[12] at 267 nm excitation the small 0.5 ps component is mostly due to keto-Cy, whereas the long component (ca. 4.5 ps) is due to enol-Cy.

With a single water molecule attached, the Cy·H_2O transient exhibits a very different behavior. In addition to the nonresonant initial spike, the rest of the temporal profile can be well described by a single exponential decay of 0.5 ps. Comparing the Cy and Cy·H_2O transients, it seems that upon monohydration the long component (ca. 4.5 ps) fades away, while the short components remain intact. For larger microhydrates, Cy·$(H_2O)_{2,3}$, the decays become even faster (ca. 0.2 ps). These observations immediately suggest an apparent excited-state lifetime shortening upon microhydration of Cy.

Interpretations of these transients must take the isomeric structures of Cy microhydrates into account. We calculated the relative energies of various Cy·$(H_2O)_{1\text{-}3}$ isomers with the G4MP2 composite method,[26] an economical version of the high-accuracy G4 theory. For comparison, we also carried out the dispersion-corrected density functional theory calculations at the ωB97XD/aug-cc-pVTZ level of theory.[27] This functional has been reported to give an excellent performance[28] for interaction energies of noncovalent molecular complexes,[29–31] including those involving H-bonding between nucleobases.[31] The energies of a few important structures were also calculated at the more expensive CCSD(T)/aug-cc-pVTZ level of theory for accuracy assessments.

Table 1 lists the relative energies of the two most stable monohydrates for each Cy major tautomers, and the ωB97XD-optimized structures of the three lowest-energy isomers are shown in Figure 1 B. A more thorough list of Cy·H_2O isomers are given in the Supporting Information. The water binding sites are denoted as **A**, **B**, and **C**, following the labeling conventions used by other authors.[32–34] For keto-Cy, site **A** is at the sugar edge, whereas sites **B** and **C** are along the Watson–Crick edge. In general, our computation results are consistent with previous studies regarding the stability order among Cy·H_2O isomers.[8,23,24,32–39] The G4MP2 energies agree very well with the more accurate CCSD(T) results. However, we found that ωB97XD fails to predict the correct stability order of the keto and enol forms of Cy monomer (see the Supporting Information), and therefore, ωB97XD results should be considered only for binding-site isomers of the same Cy tautomers.

As shown in Table 1, the stability order between the enol and keto forms of Cy microhydrates is inverted even with a single hydration water. For the binding site **A**, keto-Cy·H_2O is predicted to be more stable than enol-Cy·H_2O by 3 kJ mol^{-1} at the G4MP2 and CCSD(T)/aug-cc-pVTZ levels. Unlike in the case of Cy monomer, we believe that structural relaxations occur rapidly in Cy·$(H_2O)_n$ during expansion because of the following reasons. 1) Tautomerization barriers in Cy·

Table 1: Zero-point energy corrected relative energies (ΔE_{ZPE}) and Boltzmann populations (%) at 50, 100, and 150 K of low-energy isomers of Cy mono- and dihydrates. All energies are in kJ mol^{-1}.

Cy·$(H_2O)_n$–sites	ΔE_{ZPE}[a] G4MP2	ΔE_{ZPE}[b] ωB97XD	ΔE_{ZPE}[c] CCSD(T)	$P_{50\,K}$[d] [%]	$P_{100\,K}$[d] [%]	$P_{150\,K}$[d] [%]
keto-Cy·H_2O_A	0	0	0	98.9	86.3	70.5
keto-Cy·H_2O_B	1.96	2.28	2.70	1.0	10.3	19.6
enol-Cy·H_2O_A	2.89	9.49	3.24	< 0.1	2.43	5.89
enol-Cy·H_2O_B	3.92	10.7		ca. 0	0.94	3.77
imino-Cy·H_2O_A	8.02	13.9		ca. 0	ca. 0	0.13
imino-Cy·H_2O_B	10.3	14.6		ca. 0	ca. 0	ca. 0
keto-Cy·$(H_2O)_2$_AA	0	0		99.6	93.2	82.6
keto-Cy·$(H_2O)_2$_AB	2.39	4.20		0.25	3.7	8.52
keto-Cy·$(H_2O)_2$_BB	2.85	4.15		0.1	3.0	8.63

[a] G4MP2. [b] ωB97XD/aug-cc-pVTZ. [c] CCSD(T)/aug-cc-pVTZ//ωB97XD/aug-cc-pVTZ. [d] Boltzmann populations calculated with ΔG^0 values obtained from G4MP2 results.

$(H_2O)_{1\text{-}3}$ are greatly reduced with the assistance of water bridges to 40 kJ mol^{-1} (see the Supporting Information) or less.[23,24,39–42] 2) Isomerization barriers between different water binding sites are expected to be even lower. For example, it has been shown that the barrier between two remote H-bonding sites of the *t*-formanilide·H_2O complex is only about 12 kJ mol^{-1}.[43] 3) Small Cy microhydrates are very strongly bound because of the presence of dual H-bonds for each water. Previous studies at various levels of theory have reported hydration energies of about 40–50 kJ mol^{-1} per water molecule.[8,32–36,38,44]

These properties assure extensive structural relaxation of Cy·$(H_2O)_n$ in the Ar/H_2O expansion.[45–48] First, upon formation of metastable Cy···H_2O collision complexes in the clustering region of the expansion, the binding and collision energies can quickly flow into internal modes of the complex via rapid intramolecular vibrational-energy redistribution. Thus, the total internal energy of the complex is the sum of the binding energy, the internal energy of Cy and H_2O, and the collision energy.[45–48] Because Cy contains a substantial amount of thermal energy before complete cooling, for example 20 kJ mol^{-1} at 300 K,[49] the incipient Cy···H_2O complexes possess internal energies well above barriers to water-assisted tautomerization and binding-site isomerization. Randomization rapidly proceeds to equilibrate among all isomeric structures until the complexes are cooled to some intermediate temperatures at which barrier crossing are not feasible. Second, transient cold collisions of Cy microhydrates with water molecules (ca. 12%) in the non-clustering binary collision region can catalyze further structural relaxation and drive the distributions to equilibrium near the terminal temperatures of the expansion.[45,48] Schematic illustrations of these relaxation processes are given in the Supporting Information.

Although the true distributions among various Cy·$(H_2O)_n$ isomers are not exactly known and probably cannot be described by a single temperature, some important conclusions can still be derived by considering their equilibrium distributions within a probable range of final vibrational temperatures in the jet. In Table 1 we also listed the Boltzmann populations calculated with ΔG^0 obtained from G4MP2 results (see the Supporting Information) at three temperatures: 50, 100, and 150 K. The lower limit (50 K) is based on a previous report of similar expansion conditions,[50,51] and the higher ones are estimates accounting for possible incomplete vibrational cooling.

Within this temperature range, the keto form becomes the dominant tautomer for Cy·H_2O with a population of $>90\%$. Accordingly, we proposed that the Cy·H_2O transient is mostly due to keto-Cy·H_2O, and contributions from other tautomers are minor ($<10\%$).[52] Our calculations also predict that monohydration of keto-Cy at site **A** is more stable than at site **B** by about 2.0–2.7 kJ mol^{-1}. This result is consistent with a recent study that experimentally confirmed that 2-pyridone binds more strongly at site **A** than at site **B** of keto-Cy.[53] Because of the lower barriers involved, the distributions of binding-site isomers are expected to approach those near the low temperature limit (<100 K), suggesting that the Cy·H_2O transient arises mostly ($>90\%$) from keto-Cy·H_2O with the water bound at site **A**. An immediate conclusion is that monohydration of keto-Cy at site **A** does not alter its excited-state deactivation dynamics much, because the decay time is essentially the same as that of keto-Cy monomer at the same excitation energy.

For Cy dihydrates, our calculations predict that the keto form predominates exclusively; all other tautomeric forms of Cy·$(H_2O)_2$ are much higher in energy (see the Supporting Information). The relative energies and populations of the three lowest-energy keto-Cy·$(H_2O)_2$ isomers are also listed in Table 1. The most stable keto-Cy·$(H_2O)_2$, shown in Figure 1 B, has both water molecules bound at site **A** and is denoted as the "AA" isomer. The next two stable isomers, denoted as "AB" and "BB" isomers, are very close in energy and are about 2.4–4.2 kJ mol^{-1} higher than the "AA" isomer. As a result, the "AA" isomer dominates ($>93\%$) the dihydrate population near the low temperature limit. This assignment indicates that two-water binding at site **A** induces a stronger lifetime shortening than just a single water bound at the same site. For Cy·$(H_2O)_3$, our calculations predict two major isomers, AAB and ABB (see the Supporting Information), which dominate the trihydrates population near the low temperature limit. The Cy·$(H_2O)_3$ decay is nearly the same (ca. 0.2 ps) as that of the dihydrates, indicating that the lifetime shortening may saturate with 2–3 microhydrated water molecules.

Although the size of microhydrates studied here are rather small, it is enlightening to compare our results with those measured in the bulk. Interestingly, a very recent study[19] for Cy excited at about 267 nm in aqueous solutions has revealed an ultrafast initial decay of about 0.2 ps, which is nearly the same as the lifetimes observed here with 2–3 microhydrated water molecules. However, two slower components of 1.5 and 7.7 ps were also identified,[19] suggesting that the deactivation dynamics may be more complex in the bulk due to full hydration.

Because the N1 position is the sugar-binding site for Cy, the dominant monohydrate with a H_2O bound at site **A** is less biologically relevant. To explore the effect of hydration at site **B**, which is a more pertinent analogy to the H-bonding in the Watson–Crick base pairing, we also study microhydrates of 1-methylcytosine (1mCy). Figure 2 displays the 1mCy and 1mCy·$(H_2O)_{1,2}$ transients measured under similar conditions. 1mCy exists predominately as the keto form in the gas phase, and as such, 1mCy has often been used to identify the keto contributions in Cy tautomeric mixtures.[12,53,54] The presumption that the excited-state energetics and dynamics of 1mCy closely resemble those of keto-Cy has been discussed previously[12,54] and is supported by more recent theoretical studies.[14,15] As shown in Figure 2, the 1mCy monomer transient does exhibit the characteristic 0.5 ps decay of keto-Cy at 267 nm excitation. However, unlike the monohydrated keto-Cy, 1mCy·H_2O exhibits a markedly shorter excited-state lifetime of about 0.15 ps. Chemical intuition suggests that methyl substitution at the N1 position also makes water binding at site **A** unfavorable. Indeed, our calculations predict that the most stable structure of 1mCy·H_2O is the one with a H_2O bound at site **B**. Other isomers are at much higher energies (see the Supporting Information). Thus, the differ-

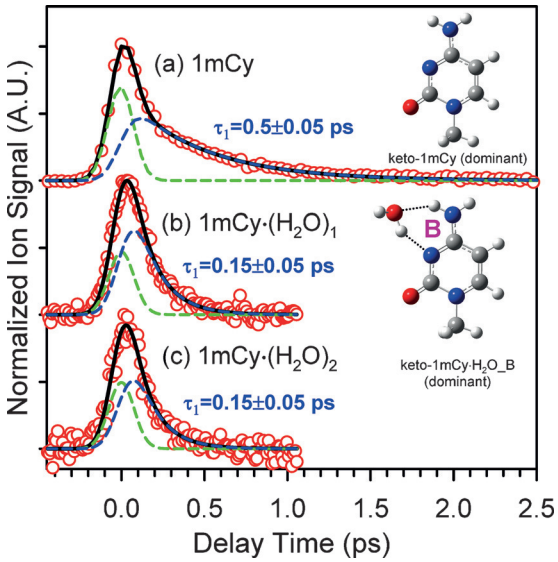

Figure 2. Mass-selected pump–probe photoionization transients ($\lambda_{pump}=267$ nm; $\lambda_{probe}=800$ nm) of 1mCy and 1mCy microhydrates: a) 1mCy monomer, b) 1mCy·H_2O, and c) 1mCy·$(H_2O)_2$. The black solid lines are the best fits with a single-exponential decay and an initial spike convoluted with the IRF (0.2 ps FWHM Gaussian). The dashed lines are the individual components obtained from the fits. The insets show the ωB97XD-optimized structures of the dominant 1mCy and 1mCy·H_2O isomers.

ence observed between the Cy·H_2O and 1mCy·H_2O transients suggests a possible hydration-site dependence, that is, monohydration at the Watson–Crick site **B** induces a substantially stronger effect than at the sugar-edge site **A** in accelerating the excited-state deactivation of keto-Cy.

The decay time scales observed here are too short for the evaporation of water molecules, that is, vibrational predissociation, and therefore, they must be interpreted with reference to the microhydration effects on the deactivation of the initially excited $^1\pi\pi^*$ state of keto-Cy. Previous theoretical studies have identified at least three deactivation pathways leading to the ground state via characteristic conical intersections (CIs).[13,55–63] The first pathway connects the Franck–Condon (FC) region to a $^1\pi\pi^*/S_0$ type CI associated with a dihedral twist around the C5-C6 bond.[55–58,63] The second pathway connects the FC region to a $^1n_N\pi^*/S_0$ type CI characterized by a N3 puckering and involves a state switch between the $^1\pi\pi^*$ and the $^1n_N\pi^*$ states.[57,58,60] A recent study has indicated that this $^1n_N\pi^*/S_0$ CI is probably better described as a $^1\pi_{N3}\pi^*/S_0$ CI with a non-negligible $^1n_N\pi^*$ contribution.[13] The third pathway goes through a semi-planar $^1n_O\pi^*/S_0$-type CI, which has been shown to be highly unfavorable because of a substantially high barrier involved.[13,57–60] The first two pathways involve similar low barriers of about 0.1–0.2 eV,[13,57–59,63] and therefore, the initially excited $^1\pi\pi^*$ state of keto-Cy probably decays competitively via these two pathways. Recent experiments have supported the presence of such low barriers.[12,16] It is likely that microhydration perturbs the energetics of these pathways, and thereby, accelerates the excited-state deactivation.

The hydration-site dependence may arise from unique perturbations at specific sites[5] and can be qualitatively understood as follows. Single-water H-bonding interaction with the nonbonding orbitals of the C=O group at site **A** may perturb the pathway via the $^1n_O\pi^*/S_0$ CI, but the effect is probably not strong enough to lower the associated high barrier to alter the dominance of the other two more important pathways, which are probably only weakly perturbed by monohydration at site **A**. On the other hand, H-bonding interaction with the nonbonding electrons on the N3 atom at site **B** directly influences the energetics of the $^1n_N\pi^*/S_0$ CI pathway, one of the major deactivation route, and therefore, is more likely to produce a stronger effect. Indeed, it has been shown that, although the vertical excitation energy of the first $^1\pi\pi^*$ states of keto-Cy is nearly invariant (< 0.1 eV for $n=1,2$) for microhydration at both sites,[33] water binding at site **B** results in a substantially larger effect than at site **A** in raising the $^1n_N\pi^*$ state energy.[33] The $^1n_N\pi^*$ pathway has also been shown to be destabilized upon monohydration at site **B**.[37] However, it should be noted that such effect does not necessarily imply an increase in the barrier height between the $^1n_N\pi^*$ and $^1\pi\pi^*$ states. A recent study at CC2/def2-TZVPPD level of theory indicated that the minimum of the first $^1n_N\pi^*$ state is lower than that of the first $^1\pi\pi^*$ state by about 0.3 eV.[64] Consequently, water binding at site **B** reduces the energy gap between the $^1n_N\pi^*$ and $^1\pi\pi^*$ states, and a barrier lowering may occur in a scenario similar to the Marcus inverted region in electron transfer reactions. (see Figure S9 in the Supporting Information) Apparently, rigorous theoretical investigations are definitely needed to elucidate the nature of such hydration-site dependence.

In summary, the present study has shown that a markedly lifetime shortening occurs upon microhydration of Cy with even a few water molecules, and the excited-state lifetimes measured here for Cy·$(H_2O)_{1\text{-}3}$ are about 0.5–0.2 ps. Comparisons between Cy·H_2O and 1mCy·H_2O transients suggested a possible hydration-site dependence, that is, monohydration at the amino Watson–Crick site induces a substantially stronger effect than at the sugar-edge site in accelerating excited-state deactivation of Cy.

Acknowledgements

This work was supported by the Ministry of Science and Technology, Taiwan, R.O.C..

Keywords: cytosine · excited-state dynamics · femtochemistry · microhydration · nucleobases

How to cite: *Angew. Chem. Int. Ed.* **2015**, *54*, 14772–14776
Angew. Chem. **2015**, *127*, 14985–14989

[1] C. E. Crespo-Hernández, B. Cohen, P. M. Hare, B. Kohler, *Chem. Rev.* **2004**, *104*, 1977–2019.
[2] C. T. Middleton, K. de La Harpe, C. Su, Y. K. Law, C. E. Crespo-Hernandez, B. Kohler, *Annu. Rev. Phys. Chem.* **2009**, *60*, 217–239.
[3] J. Peon, A. H. Zewail, *Chem. Phys. Lett.* **2001**, *348*, 255–262.

[4] Y. Nosenko, M. Kunitski, B. Brutschy, *J. Phys. Chem. A* **2011**, *115*, 9429 – 9439.
[5] S. Lobsiger, S. Blaser, R. K. Sinha, H. M. Frey, S. Leutwyler, *Nat. Chem.* **2014**, *6*, 989 – 993.
[6] S. K. Pal, A. H. Zewail, *Chem. Rev.* **2004**, *104*, 2099 – 2123.
[7] E. Westhof, *Annu. Rev. Biophys. Biophys. Chem.* **1988**, *17*, 125 – 144.
[8] S. A. Trygubenko, T. V. Bogdan, M. Rueda, M. Orozco, F. J. Luque, J. Sponer, P. Slavicek, P. Hobza, *Phys. Chem. Chem. Phys.* **2002**, *4*, 4192 – 4203.
[9] J. K. Wolken, C. Yao, F. Turecek, M. J. Polce, C. Wesdemiotis, *Int. J. Mass Spectrom.* **2007**, *267*, 30 – 42.
[10] G. Fogarasi, *J. Phys. Chem. A* **2002**, *106*, 1381 – 1390.
[11] G. Bazsó, G. Tarczay, G. Fogarasi, P. G. Szalay, *Phys. Chem. Chem. Phys.* **2011**, *13*, 6799 – 6807.
[12] J. W. Ho, H. C. Yen, W. K. Chou, C. N. Weng, L. H. Cheng, H. Q. Shi, S. H. Lai, P. Y. Cheng, *J. Phys. Chem. A* **2011**, *115*, 8406 – 8418.
[13] A. Nakayama, Y. Harabuchi, S. Yamazaki, T. Taketsugu, *Phys. Chem. Chem. Phys.* **2013**, *15*, 12322 – 12339.
[14] A. Nakayama, S. Yamazaki, T. Taketsugu, *J. Phys. Chem. A* **2014**, *118*, 9429 – 9437.
[15] Q. S. Li, L. Blancafort, *Photochem. Photobiol. Sci.* **2013**, *12*, 1401 – 1408.
[16] S. Lobsiger, M. A. T'rachsel, H. M. Frey, S. Leutwyler, *J. Phys. Chem. B* **2013**, *117*, 6106 – 6115.
[17] K. Kosma, C. Schroter, E. Samoylova, I. V. Hertel, T. Schultz, *J. Am. Chem. Soc.* **2009**, *131*, 16939 – 16943.
[18] P. M. Hare, C. E. Crespo-Hernandez, B. Kohler, *Proc. Natl. Acad. Sci. USA* **2007**, *104*, 435 – 440.
[19] C. S. Ma, C. C. W. Cheng, C. T. L. Chan, R. C. T. Chan, W. M. Kwok, *Phys. Chem. Chem. Phys.* **2015**, *17*, 19045 – 19057.
[20] L. Belau, K. R. Wilson, S. R. Leone, M. Ahmed, *J. Phys. Chem. A* **2007**, *111*, 7562 – 7568.
[21] The total photon energy deposited in the present pump–probe $1+3'$ REMPI Scheme is about 9.3 eV.
[22] Z. B. Yang, M. T. Rodgers, *Phys. Chem. Chem. Phys.* **2004**, *6*, 2749 – 2757.
[23] D. Mazzuca, T. Marino, N. Russo, M. Toscano, *J. Mol. Struct. THEOCHEM* **2007**, *811*, 161 – 167.
[24] T. Das, D. Ghosh, *J. Phys. Chem. A* **2014**, *118*, 5323 – 5332.
[25] C. G. Triandafillou, S. Matsika, *J. Phys. Chem. A* **2013**, *117*, 12165 – 12174.
[26] L. A. Curtiss, P. C. Redfern, K. K. Raghavachari, *J. Chem. Phys.* **2007**, *127*, 124105.
[27] J. D. Chai, M. Head-Gordon, *Phys. Chem. Chem. Phys.* **2008**, *10*, 6615 – 6620.
[28] For example, as reported in ref. [29], for the S22 data set containing small complexes of 8–26 atoms, which are similar in size to the present system, the mean absolute deviation of interaction energies calculated at ωB97XD/aug-cc-pVTZ with respect to the "gold standard" (CCSD(T)/CBS) values is 1.13 kJ mol^{-1} for the H-bonded subset.
[29] L. A. Burns, A. Vazquez-Mayagoitia, B. G. Sumpter, C. D. Sherrill, *J. Chem. Phys.* **2011**, *134*, 084107.
[30] K. S. Thanthiriwatte, E. G. Hohenstein, L. A. Burns, C. D. Sherrill, *J. Chem. Theory Comput.* **2011**, *7*, 88 – 96.
[31] A. Li, H. S. Muddana, M. K. Gilson, *J. Chem. Theory Comput.* **2014**, *10*, 1563 – 1575.
[32] G. Fogarasi, P. G. Szalay, *Chem. Phys. Lett.* **2002**, *356*, 383 – 390.
[33] P. G. Szalay, T. Watson, A. Perera, V. Lotrich, G. Fogarasi, R. J. Bartlett, *J. Phys. Chem. A* **2012**, *116*, 8851 – 8860.
[34] S. Thicoipe, P. Carbonniere, C. Pouchan, *J. Phys. Chem. A* **2013**, *117*, 7236 – 7245.
[35] A. K. Chandra, D. Michalska, R. Wysokinsky, T. Zeegers-Huyskens, *J. Phys. Chem. A* **2004**, *108*, 9593 – 9600.
[36] K. C. Hunter, L. R. Rutledge, S. D. Wetmore, *J. Phys. Chem. A* **2005**, *109*, 9554 – 9562.
[37] L. Blancafort, A. Migani, *J. Photochem. Photobiol. A* **2007**, *190*, 283 – 289.
[38] S. Kim, H. F. Schaefer, *J. Chem. Phys.* **2007**, *126*, 064301.
[39] H. T. Zheng, D. X. Zhao, Z. Z. Yang, *Chin. J. Chem.* **2011**, *29*, 2243 – 2248.
[40] G. Fogarasi, *Chem. Phys.* **2008**, *349*, 204 – 209.
[41] A. Furmanchuk, O. Isayev, L. Gorb, O. V. Shishkin, D. M. Hovorun, J. Leszczynski, *Phys. Chem. Chem. Phys.* **2011**, *13*, 4311 – 4317.
[42] I. G. Shterev, V. B. Delchev, *Monatsh. Chem.* **2009**, *140*, 1381 – 1394.
[43] J. R. Clarkson, E. Baquero, V. A. Shubert, E. M. Myshakin, K. D. Jordan, T. S. Zwier, *Science* **2005**, *307*, 1443 – 1446.
[44] T. van Mourik, D. M. Benoit, S. L. Price, D. C. Clary, *Phys. Chem. Chem. Phys.* **2000**, *2*, 1281 – 1290.
[45] U. Erlekam, M. Frankowski, G. von Helden, G. Meijer, *Phys. Chem. Chem. Phys.* **2007**, *9*, 3786 – 3789.
[46] J. Yao, H. S. Im, M. Foltin, E. R. Bernstein, *J. Phys. Chem. A* **2000**, *104*, 6197 – 6211.
[47] M. K. Hazra, T. Chakraborty, *J. Phys. Chem. A* **2006**, *110*, 9130 – 9136.
[48] W. Y. Sohn, M. Kim, S. S. Kim, Y. D. Park, H. Kang, *Phys. Chem. Chem. Phys.* **2011**, *13*, 7037 – 7042.
[49] $< E_{vib} >$ of keto-Cy at 300 K was calculated with ωB97X-D/aug-cc-pVTZ frequencies to be about 18 kJ mol^{-1}. Adding the translational energy makes up to about 20 kJ mol^{-1}.
[50] A. Amirav, U. Even, J. Jortner, *Chem. Phys.* **1980**, *51*, 31 – 42.
[51] It has been reported in ref. [50] that cooling of large molecules, for example, tetracene, to $T_{vib} < 50$ K can be achieved in continuous supersonic expansion of Ar with $P_0 \cdot D \approx 2.4$–3.0 torr cm at nozzle temperatures of 470–510 K, where P_0 is the stagnation pressure and D is the nozzle pinhole diameter. In our case, $P_0 \cdot D \approx 3.5$ torr cm and nozzle temperature = 500 K.
[52] The dense vibronic transitions in the high-energy region of $^1\pi\pi^*$ states and the similar oscillator strengths and ionization energies (ref. [20,33]]) of Cy microhydrates ensure that the observed ion signals are roughly proportional to their ground-state populations.
[53] J. A. Frey, P. Ottiger, S. Leutwyler, *J. Phys. Chem. B* **2014**, *118*, 682 – 691.
[54] E. Nir, M. Muller, L. I. Grace, M. S. de Vries, *Chem. Phys. Lett.* **2002**, *355*, 59 – 64.
[55] K. Tomić, J. Tatchen, C. M. Marian, *J. Phys. Chem. A* **2005**, *109*, 8410 – 8418.
[56] M. Merchán, R. Gonzalez-Luque, T. Climent, L. Serrano-Andrés, E. Rodríguez, M. Reguero, D. Peláez, *J. Phys. Chem. B* **2006**, *110*, 26471 – 26476.
[57] L. Blancafort, *Photochem. Photobiol.* **2007**, *83*, 603 – 610.
[58] K. A. Kistler, S. Matsika, *J. Phys. Chem. A* **2007**, *111*, 2650 – 2661.
[59] M. Merchán, L. Serrano-Andrés, *J. Am. Chem. Soc.* **2003**, *125*, 8108 – 8109.
[60] N. Ismail, L. Blancafort, M. Olivucci, B. Kohler, M. A. Robb, *J. Am. Chem. Soc.* **2002**, *124*, 6818 – 6819.
[61] H. R. Hudock, T. J. Martinez, *ChemPhysChem* **2008**, *9*, 2486 – 2490.
[62] M. Barbatti, A. J. A. Aquino, J. J. Szymczak, D. Nachtigallova, H. Lischka, *Phys. Chem. Chem. Phys.* **2011**, *13*, 6145 – 6155.
[63] M. Z. Zgierski, S. Patchkovskii, E. C. Lim, *J. Chem. Phys.* **2005**, *123*, 081101.
[64] V. A. Ovchinnikov, D. Sundholm, *Phys. Chem. Chem. Phys.* **2014**, *16*, 6931 – 6941.

Received: August 13, 2015
Revised: September 18, 2015
Published online: October 22, 2015

